Acoustic emulsification. Part 2. Breakup of the large primary oil droplets in a water medium

By M. K. LI† AND H. S. FOGLER

Department of Chemical Engineering, University of Michigan, Ann Arbor

A theoretical model is presented for the liquid–liquid emulsification phenomenon based on the deformation and breakup of an oil droplet exposed to a cavitation shock wave generated by an acoustic field. The model predicts a relationship between the Ohnesorge number and the critical Weber number ratio for long acoustic irradiation times. At short irradiation times, the mean particle size and variance decrease with increasing time of acoustic irradiation. The results show remarkable agreement when compared with results obtained from the studies on liquid droplets exposed to shock impact from a gas stream. The mechanism for acoustic emulsification is that large oil droplets originally formed from the instability oil–water interface are disintegrated into smaller ones by the cavitation until a critical size, characteristic of the particular oil–water system, is reached.

1. Introduction

It has been shown in part 1 (Li & Fogler 1978) that the interfacial instability hypothesis is able to model satisfactorily the initial phase of the droplet formation processes in acoustic emulsification for a given oil–water system.

However, one also observes many small droplets of the order of sub-microns in the suspension systems even at relatively short irradiation times. Furthermore, as the irradiation time increases, the concentration of the large particles decreases rapidly and the mean particle size shifts toward a smaller more stable size. After the *stable* size for a given system has been reached, further acoustic irradiation was found to have no effect on the suspension size and distribution characteristics. The stable droplet sizes found for the three oil–water systems, namely the styrene–water, octacosane–water and the hexatriacontane–water systems, are respectively 0·15, 0·22 and 0·25 μm. Meanwhile the size distributions have been observed to narrow appreciably to form a homogeneous suspension.

The interfacial instability hypothesis, which predicts a droplet size several orders of magnitude larger than the observed sub-micron droplets, is incapable of adequately accounting for the droplets present in the system at moderately short or longer irradiation times. Consequently, one needs to consider a secondary breakup mechanism where other types of force might affect the process of emulsification under the influence of an acoustic field. The cavitation-induced shock impact force which is known to be present in the ultrasonic system is a subsequent logical source for such consideration (Fogler 1971).

† Present address: General Electric Corporate Research and Development, Schenectady, New York.

In this paper, several key parameters will first be discussed in relation to their effect on the shock-wave pressure generated by the implosion of a cavitating bubble. In addition, since different stable droplet sizes are reached for the three different oil–water systems, the stable size could be related to the physical properties of the systems employed. Based on the assumptions that: (i) the viscosity of the ambient fluid will be neglected, and (ii) a pressure distribution on the oil droplet will be prescribed to correspond to the condition of a shock exposure, a model for the droplet deformation and breakup will be developed for the case of a slightly viscous oil in terms of two dimensionless quantities, the Ohnesorge number and the critical Weber number ratio. Finally, the experimental results for these oil–water systems at long irradiation times will be analysed and presented in terms of these two dimensionless quantities, and then compared with the results obtained from several gas–liquid systems where the liquid droplets are shattered by the oncoming gas shock.

2. Theory

2.1. *Effect of some important cavitation parameters*

The issue of practical importance in considering the effects of cavitation on the liquid–liquid emulsification process is the shock-wave intensity generated by the implosion of the cavitating bubbles. Benjamin (1958) studied the conditions under which a shock will form when the inward collapse of a transient cavitation bubble is arrested by the rising pressure of the gas and vapour in it. He established a relation between the maximum pressure generated within the cavity upon collapse, and the distance from the centre of the cavity at which the shock would form. Furthermore, it was shown that this maximum pressure is proportional to the shock-wave intensity on the basis of the cavitation noise spectra.

Sirotyuk extended Benjamin's work by considering the effects of temperature, dissolved gas, and static pressure on the shock-wave intensity. Since the vapour pressure increases exponentially with temperature, the higher the vapour pressure and the higher the gas content inside the bubble, the greater will be the retardation of the collapse, as Sirotyuk verified experimentally (1966a, 1971). These effects will decrease the shock-wave intensity. In addition, an increase in the hydrostatic pressure will also induce a more intense collapse, as was confirmed in the study by Sirotyuk (1966b).

2.2. *The secondary breakup process*

It it known that a liquid globule which has a translatory motion relative to the surrounding fluid can break up if the velocity exceeds a critical value (Hinze 1955). Similarly, a droplet will also break up if, at a given velocity or shock-wave intensity impinging on the droplet, the size of the globule is greater than a critical diameter. In an acoustically cavitating field, shock waves are constantly generated as a result of cavitation bubbles collapsing in a water medium (Flynn 1964). The suspended oil droplets thus are experiencing constant impact forces from these shock waves.

For a given intensity of the cavitation shock wave, large oil droplets will break up into smaller droplets which undergo further breakup until a critical droplet diameter is reached. Droplets with diameters smaller than or equal to this critical diameter will not break up further.

Acoustic wave
↓ ↓ ↓ ↓

Oil

1st stage
Increasing *t*   Water
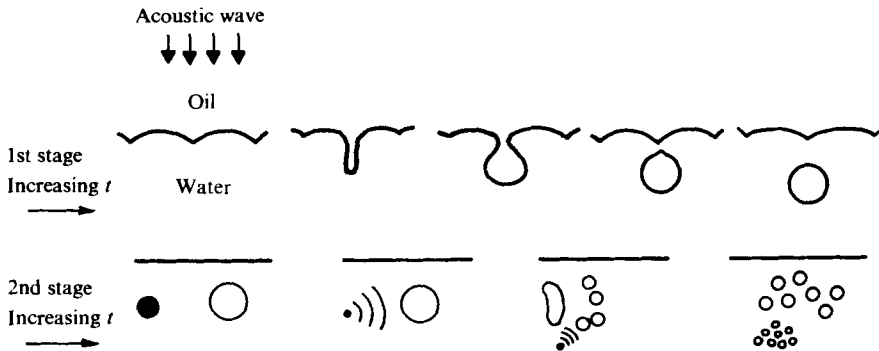
2nd stage
Increasing *t*

FIGURE 1. Acoustic emulsification mechanism.

This process of the successive disintegration of the large droplets formed initially from the instability of the oil–water interface, which continues until they reach a stable droplet size, is referred to as the secondary breakup mechanism. That is, the acoustic emulsification mechanism consists of two stages as shown schematically in figure 1.

The first stage is the incipient instability of the oil–water interface to produce large oil drops of the order of $70\,\mu\mathrm{m}$ in diameter. The second stage involves the breakup of these larger droplets by shock waves [denoted by '(('] in figure 1 produced by cavitating bubbles [denoted by the solid circle].

In discussing the fundamentals of the hydrodynamic mechanism of the breakup of the droplets in the dispersion processes, Hinze (1955) noted two parameters of practical importance, namely the Weber number N_{we} (which is the ratio of the dynamic forces acting on the droplet to the surface tension forces), and the Ohnesorge number N_{vi} (which is defined as the ratio of the viscous force to the geometric mean of the inertial and surface-tension forces). In general, the critical Weber number $(N_{we})_{\mathrm{crit}}$ (which refers to the critical value *above* which breakup occurs) depends on the type of deformation and on the flow pattern around the globule. For the case of breakup of a drop in an air stream, $(N_{we})_{\mathrm{crit}}$ varies between 13 and infinity, depending on the value of N_{vi} and on the manner in which the relative air velocity varies with time. The lower value $(N_{we}^{*} = 13)$ refers to the true shock case and an inviscid fluid, $N_{vi} \rightarrow 0$. This value may be compared with 10·3 for mercury drops in air, obtained by Haas (1964), and with 7·2 to 16·8 (with an average of about 13) for water, methyl alcohol and a low-viscosity silicone oil, obtained by Hanson, Domich & Adams (1963) in a study of droplet breakup in a shock tube. Volynski (1948) also studied the breakup of liquid droplets and his data indicated a critical Weber number of 10·6 to 14, which again agrees quite well with Hinze's value of 13.

Hinze (1948*a*, *b*) first obtained solutions of the linearized hydrodynamical equations governing the slight deformation of a globule. Formulae for the forced deformation are given for the cases of very slight and very great viscosity effects. In a subsequent paper (Hinze 1955), these results were applied to analyse the critical speeds and sizes of liquid globules and are summarized below for the oil–water system.
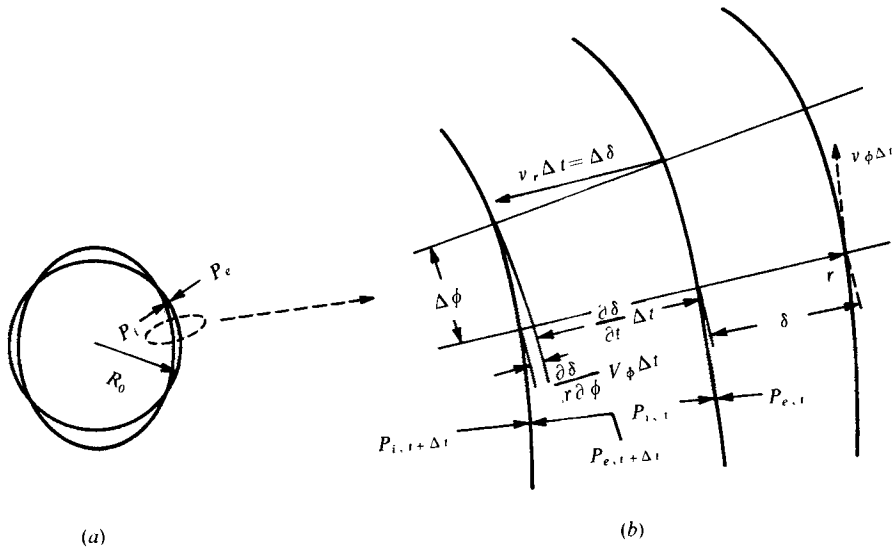
FIGURE 2. Schematic diagram of an oil droplet. (a) Deformation of the globule. (b) Relationship between v_r and the deformation of the droplet. $v_r \Delta t = (\partial\delta/\partial t)\,\Delta t + (\partial\delta/r\,\partial\phi)\,v_\varphi\,\Delta t \approx (\partial\delta/\partial t)\,\Delta t$.

2.3. General scheme of the development

Hinze (1948a) analysed liquid droplets in an air system using two-dimensional spherical co-ordinates, r and ϕ, with rotational symmetry in the θ co-ordinate. For the application of this analysis to the system of oil droplets in water, let v_r be the radial velocity component, v_ϕ the tangential velocity component and P_i the static internal pressure of the oil droplet (see figure 2). The equation of continuity and the equations of motion for the case of rotational symmetry are respectively

$$\frac{1}{r^2}\frac{\partial}{\partial r}(r^2 v_r) + \frac{1}{r\sin\phi}\frac{\partial}{\partial\phi}(v_\phi\sin\phi) = 0, \tag{1}$$

$$\rho_1\left(\frac{\partial v_r}{\partial r} + v_r\frac{\partial v_r}{\partial r} + \frac{v_\phi}{r}\frac{\partial v_r}{\partial\phi} - \frac{v_\phi^2}{r}\right) = -\frac{\partial P_i}{\partial r} + \eta_1\left(\nabla^2 v_r - \frac{2}{r^2}v_r - \frac{2}{r^2}\frac{\partial v_\phi}{\partial\phi} - \frac{2}{r^2}v_\phi\cot\phi\right), \tag{2}$$

$$\rho_1\left(\frac{\partial v_\phi}{\partial t} + v_r\frac{\partial v_\phi}{\partial r} + \frac{v_\phi}{r}\frac{\partial v_\phi}{\partial\phi} + \frac{v_r v_\phi}{r}\right) = \frac{1}{r}\frac{\partial P_i}{\partial\phi} + \eta_1\left(\nabla^2 v_\phi + \frac{2}{r^2}\frac{\partial v_r}{\partial\phi} - \frac{v_\phi}{r^2\sin^2\phi}\right), \tag{3}$$

where $\eta_1, \rho_1 =$ viscosity and density of oil respectively ($\rho_1 =$ const).

To obtain an explicit relationship for the response and deformation of a globule (when exposed to shock) for a prescribed external pressure, (1)–(3) can first be simplified by assuming the velocity components are small. After the elimination of the tangential velocity component v_ϕ, the deformation δ can then be implicitly expressed as a function of the internal static pressure of the oil droplet P_i:

$$\frac{\partial\pi_i}{\partial\epsilon} = -\left\{\frac{\partial}{\partial\tau} - N_1\left[\frac{\partial^2}{\partial\epsilon^2} + \frac{4}{\epsilon}\frac{\partial}{\partial\epsilon} + \frac{2}{\epsilon^2} + \frac{1}{\epsilon^2\sin\phi}\frac{\partial}{\partial\phi}\left(\sin\phi\frac{\partial}{\partial\phi}\right)\right]\right\}\frac{\partial\bar\delta}{\partial\tau}, \tag{4}$$

with

$$\left[\frac{1}{\epsilon^2}\frac{\partial}{\partial\epsilon}\left(r\frac{\partial}{\partial\epsilon}\right) + \frac{1}{\epsilon\sin\phi}\frac{\partial}{\partial\phi}\left(\sin\phi\frac{\partial}{\partial\phi}\right)\right]\pi_i = 0, \tag{5}$$

resulting from the equations of motion and the equation of continuity.

These equations are now written in dimensionless form using the following definitions:

$$\epsilon = r/R_0, \qquad\qquad \pi = PT_n^2/\rho_1 R_0^2,$$
$$\zeta = \delta/R_0, \qquad\qquad N_1 = \eta_1 T_n/\rho_1 R_0^2,$$
$$\tau = t/T_n, \qquad\qquad N_2 = \sigma T_n^2/\rho_1 R_0^3,$$
$$u = v T_n/R_0,$$

and

$$T_n = 2\pi \left(\frac{\rho_1 R_0^3}{(n-1)\, n(n+2)\, \sigma} \right)^{\frac{1}{2}},$$

where

R_0 = radius of the undeformed oil droplet,

σ = apparent interfacial tension,

n = harmonic order,

ρ_2 = density of the ambient fluid,

ρ_1 = density of the oil.

Since (4) and (5) pertain to the internal relations between static pressure, viscous stresses and inertial forces for the liquid droplet, the solutions of these equations have to satisfy the following boundary conditions:

(i) No displacement at the centre of the globule,

$$\zeta = 0 \quad \text{at} \quad \epsilon = 0$$

(we assume axial symmetry for the external pressure distribution).

(ii) No tangential stress, i.e.

$$\pi_{r\phi} = N_1 \left[\epsilon\, \frac{\partial}{\partial \epsilon}\, \frac{u_\phi}{\epsilon} + \frac{1}{\epsilon}\, \frac{\partial u_r}{\partial \phi} \right] = 0,$$

$$\left[\frac{1}{\epsilon^2 \sin\phi}\, \frac{\partial}{\partial\phi} \left(\sin\phi\, \frac{\partial}{\partial\phi} \right) - \frac{\partial}{\partial\epsilon} \left(\frac{1}{\epsilon^2}\, \frac{\partial}{\partial\epsilon}\, \epsilon^2 \right) \right] \frac{\partial\zeta}{\partial\tau} = 0.$$

(iii) Continuity of the normal stresses at the interface, i.e.

$$\pi_{rr} + \pi_\sigma + \pi_e = 0,$$

where

π_{rr} = internal total stress component in the radial direction (dimensionless),

π_σ = stress resulting from the interfacial tension (dimensionless),

and

π_e = external pressure acting on the surface of drop (dimensionless).

Employing the technique of the separation of variables, ζ and π_i can be further expressed as functions of the form of $f(\tau)\, g(\epsilon)\, h(\phi)$. Finally, by assuming that the external pressure distribution on the interface of the oil droplet can be expressed in zonal harmonics, $\pi_n(\cos\phi)$ (Lamb 1945, p. 123), the functions $f(\tau)$, $g(\epsilon)$, $h(\phi)$ can be evaluated from the equations of motion and the dynamic conditions, through which the prescribed external pressure is related to the internal pressure.

Analytical solutions for the deformation of the oil droplet have been obtained by Hinze for the cases where the oil considered is either slightly viscous or highly viscous (1948b), and are presented below.

Slightly viscous case. The expression for the deformation of the globule in this case is

$$\frac{\delta}{R_0} = -\frac{\rho_2 U_0^2 R_0}{\sigma} \left[0 \cdot 069 \left(1 - \exp\left\langle -\frac{\{2\eta_1}{\rho_1 R_0^2} t \right\rangle \cos\omega_2 t \right. \right.$$
$$+ 0 \cdot 021 \left(1 - \exp\left\langle -\frac{6\eta_1}{\rho_1 R_0^2} t \right\rangle \cos\omega_3 t \right)$$
$$\left. + 0 \cdot 005 \left(1 - \exp\left\langle -\frac{12\eta_1}{\rho_1 R_0^2} t \right\rangle \cos\omega_4 t \right) + \ldots \right], \tag{6}$$

where

$t = $ time after initial contact of the oil globule with the shock-wave front,

$\omega = 2\pi/T_n$.

It can be shown that the absolute maximum value of δ/R_0 in (6) which can be reached roughly for $\omega_2 t \approx 0 \cdot 8\pi$ (Littaye 1943) is

$$\left(\frac{\delta}{R_0}\right)_{max} = -\tfrac{1}{2} N_{we} [0 \cdot 095 + 0 \cdot 055 \exp(-0 \cdot 8\pi N_{vi}) + 0 \cdot 02 \exp(-2 \cdot 4\pi N_{vi}) + \ldots], \tag{7}$$

where
$$N_{vi} = \eta_1/(\rho_1 \sigma D_0)^{\frac{1}{2}} = \text{Ohnesorge number},$$
$$N_{we} = \rho_2 U_0^2 D_0/\sigma = T_d D_0/\sigma = \text{Weber number},$$

$T_d = $ dynamic pressure produced by cavitation shock wave.

Therefore, the maximum deformation ratio for an inviscid situation (i.e. $N_{vi} = 0$) is

$$\left(\frac{\delta}{R_0}\right)^*_{max} = -0 \cdot 085 N^*_{we}. \tag{8}$$

If one assumes that (i) the maximum deformation of a liquid globule, $(\delta/R_0)_{max}$, corresponds to the critical deformation, $(\delta/R_0)_{crit}$, i.e. the point at which the globule will break up, and (ii) the critical deformation for the inviscid case and the slightly viscous case are roughly the same, i.e. $(\delta/R_0)_{crit} \sim (\delta/R_0)^*_{crit}$, then we can combine (7) and (8) in the form (Li 1976):

$$\left(\frac{N_{we}}{N^*_{we}}\right)_{crit} = \frac{0 \cdot 17}{(0 \cdot 095 + 0 \cdot 055 \exp(-0 \cdot 8\pi N_{vi}) + 0 \cdot 02 \exp(-2 \cdot 4\pi N_{vi}) + \ldots)}, \tag{9}$$

for $N_{vi}^2 \ll 1$.

Thus it is seen that the critical Weber number ratio for a slightly viscous liquid globule is singly dependent on the Ohnesorge number N_{vi}.

Highly viscous case. The expression for the deformation of the globule for this case is (Hinze 1948b)

$$\frac{\delta}{R_0} = -\frac{\rho_2 U_0^2 R_0}{\sigma} \left[0 \cdot 069 \left(1 - \exp\left\langle -\frac{20\sigma}{19\rho_1 R_0} t \right\rangle \right) \right.$$
$$+ 0 \cdot 021 \left(1 - \exp\left\langle -\frac{35\sigma}{22\rho_1 R_0} t \right\rangle \right)$$
$$\left. + 0 \cdot 005 \left(1 - \exp\left\langle -\frac{36\sigma}{17\rho_1 R_0} t \right\rangle \right) + \ldots \right], \tag{10}$$

the maximum deformation $(\delta/R)_{max}$ amounts to

$$(\delta/R_0)_{max} = -0 \cdot 0475 N_{we}, \tag{11}$$

as $t \to \infty$.

As a first approximation, if one assumes that (i) the time needed for the critical deformation of the globule to be reached in this case is the same as in the slight viscosity case, i.e. at $\omega_2 t \approx 0.8$, and (ii) the critical deformation $(\delta/R_0)_{\mathrm{crit}}$ in this case is approximately equal to $(\delta/R_0)^*$ [cf. (8)], then, from (10) and (8), we have (Li 1976)

$$\left(\frac{N_{we}}{N_{we}^*}\right) = \frac{0.17}{\left[0.069\left(1-\exp\left\langle-\dfrac{4\pi}{19N_{vi}}\right\rangle\right)+0.021\left(1-\exp\left\langle-\dfrac{7\pi}{22N_{vi}}\right\rangle\right)\right.}$$
$$\left.+0.005\left(1-\exp\left\langle\dfrac{-7\cdot2\pi}{17N_{vi}}\right\rangle+\dots\right]\right. \tag{12}$$

Therefore, from an estimated value of t, the model suggests that, for indefinitely increasing N_{vi}, the value of $(N_{we}/N_{we}^*)_{\mathrm{crit}}$ and hence $N_{we,\,\mathrm{crit}}$ will increase without bound.

In the above analysis the response of the surrounding fluid to the subsequent droplet deformation is not taken into account and the normal stress acting on the droplet surface has to be prescribed during the entire period of deformation. In addition, the shear stress on the surface is assumed to be zero. In this connexion, Taylor & Acrivos (1964) have worked out an exposition of the steady-state theory of the droplet deformation in the low Reynolds number range. They showed that the deformation can be expressed by

$$\left(\frac{\delta}{R_0}\right) = -\frac{N_{we}P_2(\cos\phi)}{8(\kappa+1)^3}\left[\left(\frac{81}{80}\kappa^3+\frac{57}{20}\kappa^2+\frac{103}{40}\kappa+\frac{3}{4}\right)-\frac{\lambda-1}{12}(\kappa+1)\right], \tag{13}$$

where
$$\kappa = \eta_1/\eta_2 = \text{ratio of the viscosities,}$$
$$\lambda = \rho_1/\rho_2 = \text{ratio of the densities.}$$

A more complete analysis for the slight deformation of a liquid droplet has been treated by Chiu (1969) in which Taylor & Acrivos' result, (13), is shown to be a special case in the low Reynolds number range.

For the case of large oil viscosity as compared with the ambient fluid viscosity, i.e. κ large, Taylor & Acrivos' analysis gives

$$(\delta/R_0)_{\max} \sim -0.125N_{we}. \tag{14}$$

For the slightly viscous liquid globule exposed to a shock wave, Taylor & Acrivos' results give

$$(\delta/R_0)_{\max} \sim -0.112N_{we}, \tag{15}$$

for $\kappa \to 1$, say, as in the liquid–liquid system with similar viscosities. This result compares closely with that given by (8).

Equations (14) and (15) cover the spectrum that exists for a given system where the liquid droplet responds to the flow of an immiscible ambient fluid. Equation (14) represents the case of a liquid globule situated in a gas medium, and (15) represents the case of a liquid globule being exposed to a liquid stream. For the liquid–liquid system (say, with $\kappa = 1$), the deformation $(\delta/R_0)_{\max}$ is $-0.112N_{we}$ and the maximum error that could be carried into the result by assuming that the liquid–liquid system is approximated by a gas–liquid system is roughly 10 %.

In Hinze's development (1948a) for the case of a slightly viscous liquid globule exposed to the shock in a *gas stream*, an equation identical to (7) was obtained by ignoring the gas stream viscosity. Using the same analogy as stated in the previous
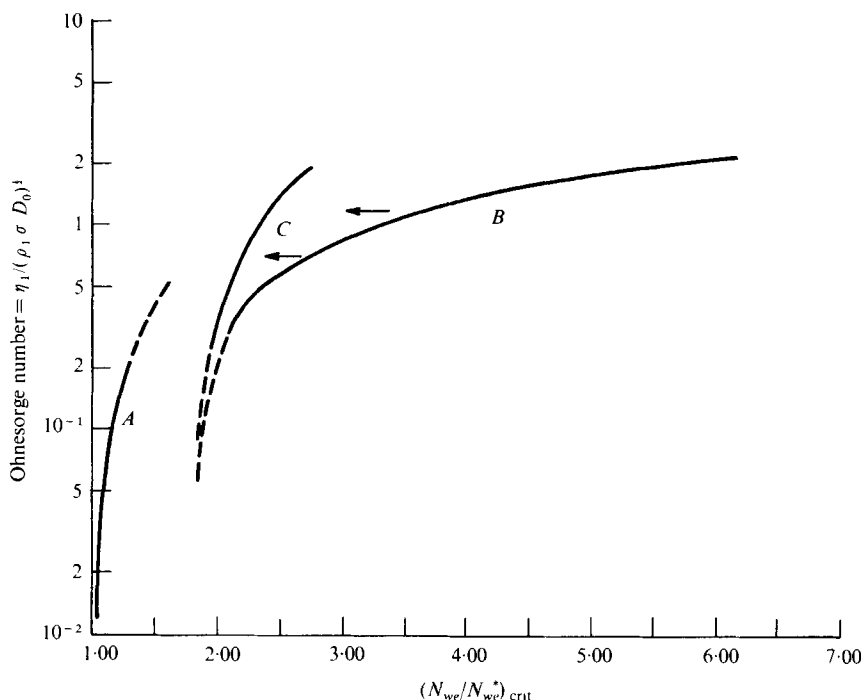
FIGURE 3. Theoretical values of Ohnesorge number as a
function of Weber number ratio.

paragraph, the error that could be associated with the assumption of inviscid ambient fluid in the case of a liquid–liquid system under shock exposure as done in the present analysis should not be overwhelming. Thus the analysis of the present liquid–liquid system based on a similar approach to Hinze's can be justified.

Figure 3 shows a plot of the Ohnesorge number *vs.* the critical Weber number ratio for both the slight (curve *A*) and the high viscosity (curve *B*) cases based on (9) and (12) respectively. It should be noted, however, that the actual time required to break up a highly viscous oil droplet could be longer. Also shown on this figure is the relation derived by Hinze (1955) (curve *C*). Unfortunately, the preparation conditions were not specified and the curve cannot be verified from the equations that Hinze presented.

3. Discussion and summary of results

From the interfacial instability hypothesis, it has been determined that, once the instability criterion is met, the oil–water interface will become unstable. The droplets resulting from the eruption of the oil phase into the water medium are related to the excited capillary wavelength λ:

$$D^* = 1 \cdot 882 \kappa_2 \lambda.$$

For the cases of monomer styrene–water, octacosane–water or the hexatriacontane–water systems, the droplet diameters should be of the order of $70 \mu m$. This view is substantiated from the experimental findings for short irradiation times.

As the oil-in-water droplets are irradiated for longer times, one can follow the reduction in particle size using the experimental techniques previously discussed (Li &
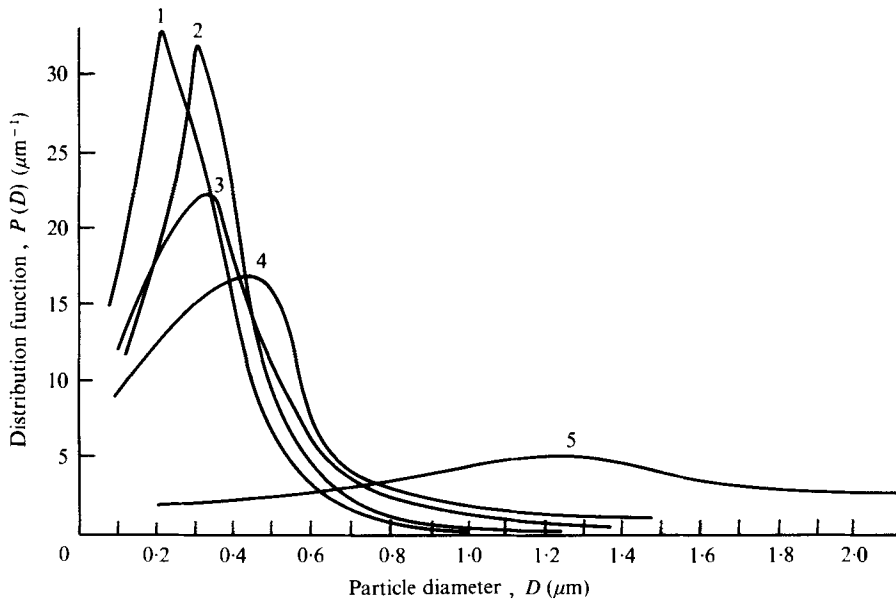
FIGURE 4. Normalized particle size distribution for $C_{28}H_{58}$–H_2O system at 72·4 °C. Oil/water ratio = 0·01/20. 1, 15·00 min; 2, 2·00 min; 3, 0·10 min, 4, 0·05 min; 5, 0·03 min.

Fogler 1978) in which the liquid particles are solidified and examined under a scanning electron microscope. The overall particle size distribution for each oil–water system shows a shift toward a smaller particle size and a more homogeneous distribution as the irradiation time increases. Typical results are shown in figures 4, 5, 8, where the particle size distribution functions $P(D)$ of the three oil–water systems are plotted as a function of the irradiation time. The quantity $P(D)\,dD$ represents the fraction of particles with diameters between D and $D + dD$. In figure 4, curve 5 represents the particle size distribution of the octacosane–water system for an irradiation time of 0·03 min. The most frequently occurring particle diameter D is 1·3 μm as indicated from the curve. The standard deviation s is found to be 1·6 μm from the particle size distribution data. As the irradiation time increases (shown by curves 4, 3, 2 and 1 respectively) the value of the mode diameter D is not only shifted toward a smaller value, but the breadth (s) of the distribution narrows as well. The values of the most frequently occurring particle diameter D, the mean diameter $\bar{D}$, and the standard deviation for the various curves represented in figure 4, along with other data, are summarized in table 1.

Figure 5 shows a similar decrease in mean particle size with increased irradiation time for the styrene–water system, although the stable droplet size is reached in a much shorter time. One can observe the extremely narrow particle size distribution from figures 6 (plate 1) and 7 (plate 2) which show typical photomicrographs of the particles after irradiation times of 0·03 min and 5 min respectively. Figure 8 shows the shift in the particle size distribution with time for the hexatriacontane–water system and figure 9 (plate 3) is a photomicrograph of these particles after 0·03 min of 20 kHz acoustic irradiation.

From these particle size distribution plots, it can be seen that certain desired suspension properties for a given oil–water system (of a specific particle size D, and

Figure 4 curve no.	Irradiation time (min)	Mode diameter D (μm)	Mean diameter $\bar{D}$ (μm)	Standard deviation s (μm)
1	15·00	0·22	0·311	0·226
	5·00	0·24	0·299	0·209
2	2·00	0·32	0·323	0·211
	0·50	0·30	0·291	0·214
3	0·10	0·34	0·438	0·386
4	0·05	0·46	0·603	0·633
5	0·03	1·30	2·093	1·603

TABLE 1. Most frequently occurring particle diameter, the mean diameter, and the standard deviation at various irradiation times for the $C_{28}H_{58}$–H_2O system.
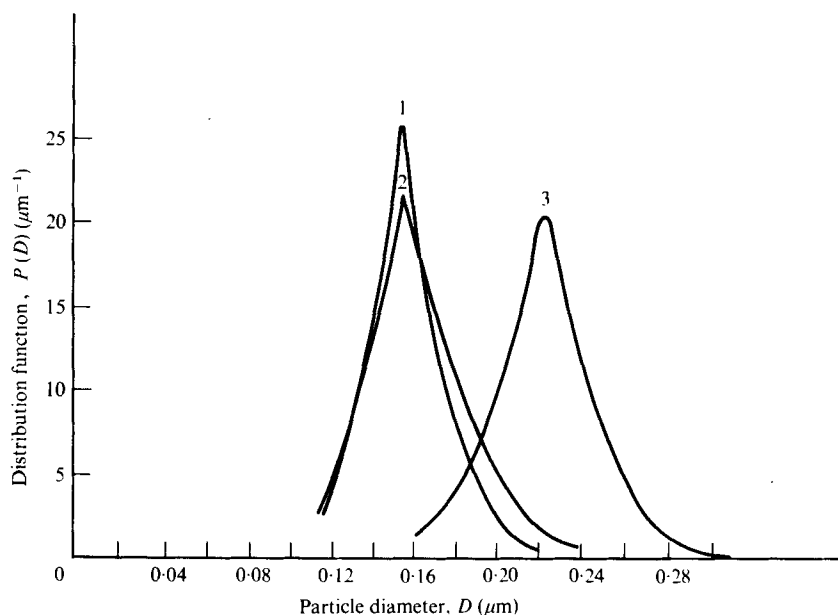
FIGURE 5. Normalized particle size distribution for styrene–water at 72·4 °C.
1, 5·00 min; 2, 1·00 min; 3, 0·03 min.

standard deviation s) may be obtained by singly controlling one variable, namely the irradiation time. However, when the same system has been irradiated beyond 15·00 min (e.g. as in the octacosane–water system), the mean particle size D, and the particle size distribution remain unchanged. This limiting diameter D implies that, once a particle reaches this size, it will not undergo further breakup. For the octacosane–water, the hexatriacontane–water, and the monomer styrene–water systems, the irradiation times needed to achieve this limiting value are approximately 15·00 min, 15·00 min, and 5·00 min.

The arithmetic mean diameters of the typical octacosane–water system as functions of the irradiation time are plotted in figure 10. This plot also accentuates the rapid disintegration processes occurring in the suspension systems, and the limiting arithmetic mean diameters at long irradiation times for the same three systems are $\sim$ 0·16, 0·31 and 0·35 μm.
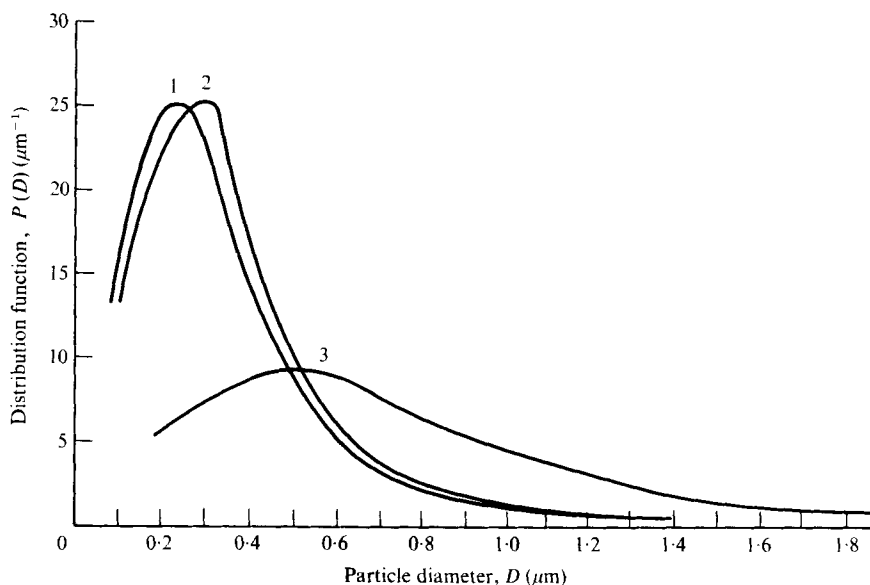
FIGURE 8. Normalized particle size distribution for $C_{36}H_{74}$–water system at 76·5 °C. 1, 15·00 min; 2, 0·05 min; 3, 0·03 min.
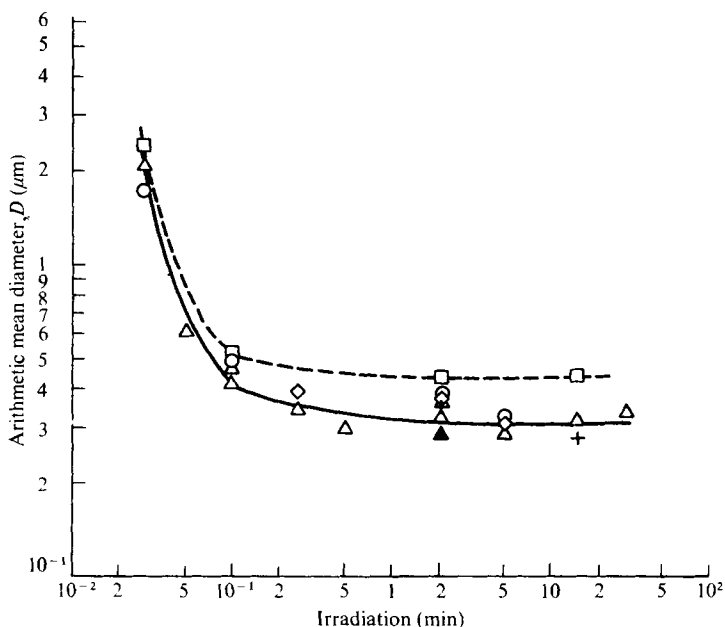

FIGURE 10. Mean diameter $\bar{D}$ as a function of irradiation time for $C_{28}H_{58}$–H_2O system at 72·4 °C. Intensity level 8 – oil/water, 0·01/20: ▲, 62·5 °C; △, 72·4 °C; +, 80·6 °C; □, 89·0 °C; oil/water, 0·10/20: ○, 72·4 °C. Intensity level 2 – oil/water, 0·01/20: ◇, 72·4 °C.

Method of analysis

Since different stable droplet diameters are observed for the three different oil–water systems at long irradiation times, the disintegration of the oil droplets should be more than a *random* process. Yet the formulation and the analysis of the deformation of an

oil droplet in a liquid–liquid system is expected to be very involved, perhaps not even tractable. Therefore, based on the reasonable assumption that the viscosity of the continuous phase can be neglected, the present system and the formulation of the problem can be simplified to that considered and obtained by Hinze (1948a, b) and Li (1976) as presented in § 2. In particular we shall calculate the Ohnesorge number and critical Weber number ratios for each of the oil–water systems and compare them with the theoretical equations and curves presented in figure 3.

First, we recall that (9) was derived for a droplet breakup under shock exposure using two major assumptions, namely: (i) the viscosity of the ambient fluid is ignored, and (ii) the viscosity of the oil droplet is small ($N_{vi}^2 \ll 1$). Of the three systems studied, the styrene–water system is the only one to have satisfied the above conditions completely. The quantity $(N_{we}/N_{we}^*)_{crit}$ may be determined for the styrene–water system from (9), i.e.

$$(N_{we}/N_{we}^*)_{crit} = 0\cdot17/(0\cdot095 + 0\cdot055^{-0\cdot8\pi N_{vi}} + 0\cdot02^{-2\cdot4\pi N_{vi}} + \ldots),$$

where $N_{vi} = \eta_1/(\rho_1 D_0 \sigma)^{\frac{1}{2}}$, for a given critical diameter D_0.

Attention now must be focused on determining the critical diameter D_0. In studies on the shattering of liquid drops by shock waves in an air stream, Hanson *et al.* (1963) were able to determine this critical diameter by exposing droplets of varying diameters to approximately the same shock intensity. The minimum droplet diameter that was able to break up at a given intensity was referred to as the critical diameter. For the present liquid–liquid system, one observes that the particle size distribution narrows and that the mode diameter D continues to decrease until it approaches a stable value after long irradiation times. This value of mode diameter after long irradiation times can be taken as the critical diameter D_0. Using this value, the Ohnesorge number for the styrene–water system is $0\cdot216$ and the critical Weber number ratio is then calculated from (9) to be $1\cdot3$. Another convenient quantity which may be used to represent the critical diameter is the mean diameter $\bar{D}$, which is noted to approach a stable value at long irradiation times (figure 10).

For each of the oil–water systems, there is a unique critical Weber number, above which value droplets of a given size will break up. This Weber number can be exceeded if the dynamic pressure T_d existing in the surrounding medium is greater than the critical value. The quantity T_d, being proportional to the square of the relative velocity between the droplet and the ambient fluid, is a function of the shock-wave intensity generated from the collapsing bubble in the surrounding medium. Taking the ratio of the critical Weber number for two oil–water systems (e.g. the styrene–water and the octacosane–water systems), one obtains from the definition of the Weber number

$$\frac{N_{we\,1}}{N_{we\,2}} = \frac{N_{we\,1}/N_{we}^*}{N_{we\,2}/N_{we}^*} = \frac{T_{d1}D_{01}/\sigma_1}{T_{d2}D_{02}/\sigma_2}. \tag{16}$$

When the operating system temperatures and pressures for the two cases are identical, the shock-wave intensities, and hence the two dynamic pressures T_{d1} and T_{d2}, are the same. Thus after rearrangement, (16) may be further simplified to

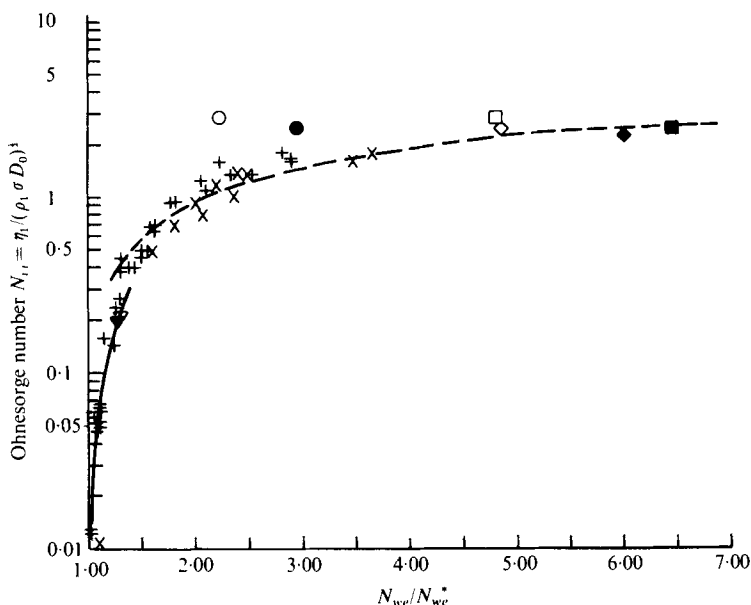$$(N_{we\,2}/N_{we}^*) = (N_{we\,1}/N_{we}^*)\frac{D_{02}\sigma_1}{D_{01}\sigma_2}. \tag{17}$$

FIGURE 11. Comparison of experimental and theoretical values of Ohnesorge number as a function of critical Weber number ratio. 72·4 °C, styrene–water: ▼, $\bar{D}$; ▽, D. 76·5 °C, $C_{36}H_{74}$–water: ●, $\bar{D}$; ○, D. 80·6 °C, $C_{28}H_{58}$–water: ◆, $\bar{D}$; ◇, D. 72·4 °C, $C_{28}H_{58}$–water: ■, $\bar{D}$; □, D. ——, stability equation; – – –, Brodkey's correlation; ×, data of Hanson *et al.*; +, data of Hinze.

Therefore, knowing the value of $N_{we\,1}/N_{we}^*$ for one oil–water system (e.g. the styrene–water system) will enable one to relate this value to $N_{we\,2}/N_{we}^*$ for another oil–water system at identical operating conditions.

On the basis of the mode diameter D, *and* the arithmetic mean diameter $\bar{D}$, for the styrene–water system at 72·4 °C, the corresponding critical Weber number ratios and the Ohnesorge numbers N_{vi} for the octacosane–water system at 72·4 °C and 80·6 °C, and the hexatriacontane–water system at 76·5 °C, respectively, are computed from (17) and plotted in figure 11 as N_{vi} vs. $(N_{we}/N_{we}^*)_{\text{crit}}$. The dynamic pressures T_d over this narrow temperature variation have been taken to be the same.

The physical property data used in evaluating the quantities N_{vi} and $(N_{we}/N_{we}^*)_{\text{crit}}$ have been either verified in the laboratory when published data are available or simply determined experimentally when this was not the case. The measured values agreed well with the estimated values except for the apparent interfacial tension of octacosane–water. In this case a value of only about 10 dynes/cm was recorded and verified by repeated measurements, which seems to be somewhat lower than expected as a result of the trace impurities present in the octacosane.

From the definition of the Weber number, it can readily be shown that the critical Weber number ratio does not involve the physical properties of either the oil droplet or the ambient fluid, but is dependent upon the relative velocity between the droplet and the surrounding medium (Li 1976). From this consideration, the results of the present study are compared with the experimental data of the gas–liquid systems obtained by Hanson *et al.* (1963) and by Hinze (1955). In addition to the experimental data, the curves based on (9) and (12) (see figure 3) along with a correlation by Brodkey (1967),

$$(N_{we}/N_{we}^*)_{\text{crit}} = 1 + 1\cdot077(N_{vi})^{1\cdot6}, \tag{18}$$

using the data of Hanson *et al.* (1963) are presented for several gas–liquid systems in figure 11 in the form of N_{vi} as a function of $(N_{we}/N_{we}^*)_{crit}$.

The results from the present liquid–liquid emulsification systems agree remarkably well with the data of Hanson and Hinze and the corresponding empirical relation based on the gas–liquid systems [equation (18)]. The implication is not only that the liquid–liquid system behaves similarly to the gas–liquid system under shock exposure, but that, because of this similarity, liquid–liquid suspension characteristics (i.e. $\bar{D}$, D) for a given system may be determined in an *a priori* manner based on this empirical correlation, should the suspension be formed by the use of acoustic means at identical conditions. In both liquid–gas and the liquid–liquid breakup processes the viscosities of the continuous phases are small compared with that of the dispersed phase.

General remarks

The effects and trends of several important parameters, namely the irradiation time, temperature and the dimension of the irradiation vessel, will be summarized in relation to the dependent variables, such as the arithmetic mean, the Sauter mean, and the standard deviation, of the suspension systems. The values of these parameters are either computed from the particle size distributions, or directly from the SEM visual screen studies (Li 1976).

Irradiation time

Irradiation time has been studied most extensively over the range of 0·03 to 30·00 min, and the suspension characteristics are found to be greatly influenced by this parameter. At short irradiation times, the size distribution of the suspension is broad with the presence of relatively many large droplets (60 μm and above), whereas the standard deviation drops rapidly with increasing irradiation, suggesting a rapid disintegrating and homogenizing action of the large droplets by the cavitation in the suspension system.

Temperature

Emulsions produced at higher temperatures yield suspensions with larger Sauter mean diameters (smaller specific surface areas) over the temperature range of 70–90 °C. These observations are in qualitative agreement with what is theoretically expected where the viscosity and intensity of collapse of the cavitation bubbles decrease with increasing temperature. This will in turn cause a diminution of the effective dynamic pressure T_d experienced by the droplet from the shocks, thereby producing particles with larger critical diameters. For the octacosane–water system at 89·0 °C, the mean diameter at long irradiation reaches a stable size of 0·44 μm compared with 0·31 μm at 72·4 °C. In general therefore the net effect of increasing temperature over this range will tend to decrease the efficiency of droplet disintegration for a given irradiation length.

Several runs at ~ 10 °C were carried out for the monomer styrene–water system. At sufficiently long irradiation times (15·00 min) it was observed that the limiting mean droplet size was about 0·10 μm compared with 0·16 μm for runs conducted at 72·4 °C. Figure 12 (plate 4) shows the typical photomicrographs of the polymerized styrene droplets at these two temperatures. At 10 °C the viscosity of water is greater than the viscosity of styrene. In addition, the collapse of the cavitation bubbles will also be

affected at these lower temperatures. Emulsification at these lower temperatures is an area for further study.

Cell dimensions

Limited studies of the styrene–water system employing different types of irradiation cells did not indicate any difference in the resulting mean particle sizes or the size distributions. However, the geometry of the irradiation system should affect the transient stage of emulsification in order to be consistent with the secondary breakup mechanism and the concept of 'cavitation zone' (Sirotyuk 1971; Rozenberg 1971). Should the cell geometry be such that the cavitation zone encompasses the entire oil–water suspension, then it is expected that the secondary breakup processes will proceed very rapidly and the stable droplet size be reached at a relatively shorter irradiation time.

4. Summary

A two-step mechanism has been proposed to explain acoustic emulsification. The first stage is the formation of large droplets by the rupture of waves on a planar interface. In the second stage the larger droplets are continually broken into smaller droplets by the collapse of cavitation bubbles. Both the mean particle size and variance decrease with increasing acoustic irradiation time. Ultimately a stable droplet size is reached after long irradiation times when the surface forces balance the inertial forces. One can derive the relationship between the Ohnesorge number and the Weber number from first principles. These two parameters are used to correlate the data. The correlation shows that the data for the breakup of liquid drops in another liquid are coincident with data obtained for the breakup of liquid droplets suspended in an air shock wave.

REFERENCES

BENJAMIN, T. B. 1958 *2nd Symp. on Naval Hydrodyn. ACR*-38 (ed. R. D. Cooper), p. 207, Office of Naval Research, Washington, D.C.

BRODKEY, R. S. 1967 *The Phenomena of Fluid Motions*. Addison-Wesley.

CHIU, H. H. 1969 *Dynamics of Deformation of Liquid Drops, Aerospace Research Laboratories Rep.* no. 69–0065.

FOGLER, H. S. 1971 *Chem. Engng Prog. Symposium Series*, vol. 67, no. 109, p. 1.

FLYNN, H. G. 1964 In *Physical Acoustic*, vol. IB (ed. W. P. Mason), p. 57. Academic Press.

HAAS, F. C. 1964 *A.I.Ch.E. J.* **10**, 920.

HANSON, A. R., DOMICH, E. G. & ADAMS, H. S. 1963 *Phys. Fluids* **6**, 1070.

HINZE, J. O. 1948a *Appl. Sci. Res.* **A1**, 263.

HINZE, J. O. 1948b *Appl. Sci. Res.* **A1**, 273.

HINZE, J. O. 1955 *A.I.Ch.E. J.* **1** 289.

LAMB, H. 1945 *Hydrodynamics*. Dover.

LI, M. K. 1976 Ph.D. thesis, The University of Michigan.

LI, M. K. & FOGLER, H. S. 1978 *J. Fluid Mech.* **88**, 499.

LITTAYE, G. 1943 *C.R. Acad. Sci. Paris* **217**, 340.

ROZENBERG, L. D. 1971 *High Intensity Ultrasonic Field.* Plenum.

SIROTYUK, M. G. 1966*a* *Sov. Phys. Acoust.* **12**, 67.

SIROTYUK, M. G. 1966*b* *Sov. Phys. Acoust.* **12**, 199.

SIROTYUK, M. G. 1971 *High Intensity Ultrasonic Field* (ed. L. D. Rozenberg). Plenum.

TAYLOR, T. D. & ACRIVOS, A. 1964 *J. Fluid Mech.* **18**, 466.

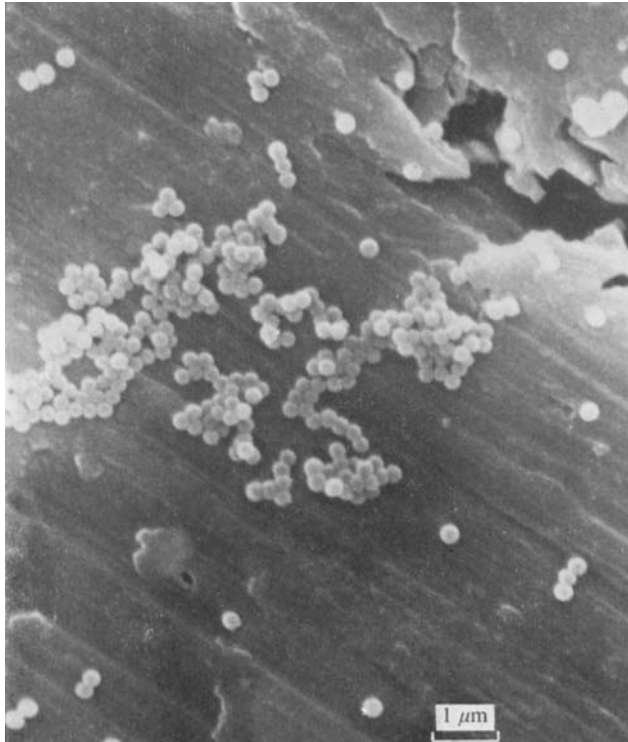VOLYNSKI, M. S. 1948 *C. R. (Doklady), Acad. Sci. U.S.S.R.* **62**, 301.

FIGURE 6. Photomicrograph cf particles for styrene–water system at
72·4 °C and after 0·03 min irradiation. $\bar{D} = 0.22\ \mu$m.

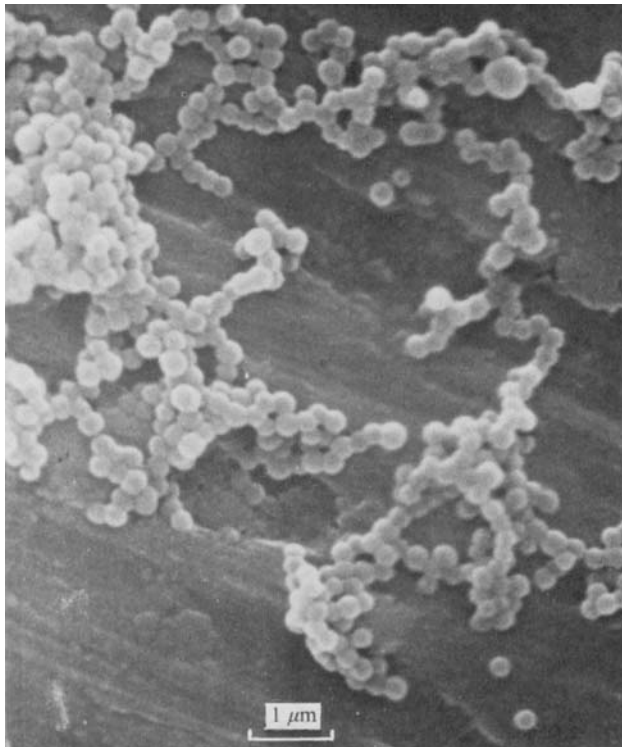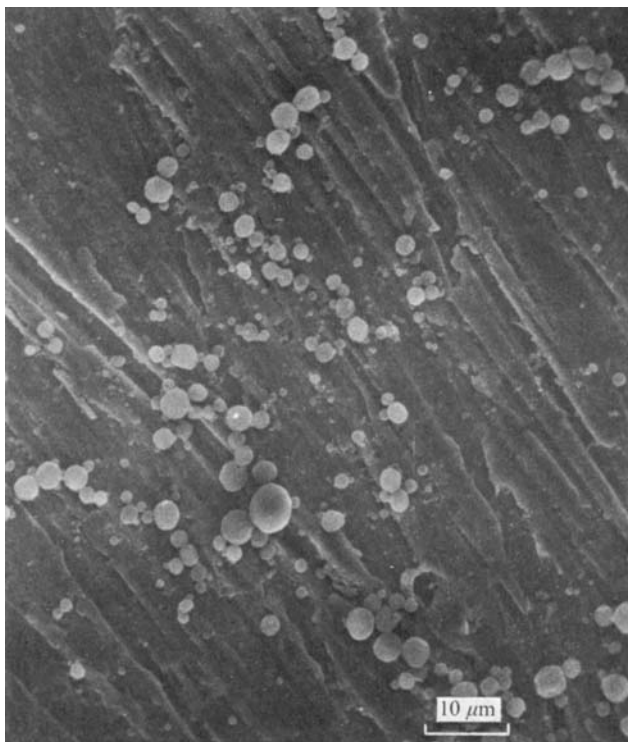FIGURE 7. Photomicrograph of particles for styrene–water system at 72·4 °C and after 5 min irradiation. $\bar{D} = 0·16$ μm.

LI AND FOGLER

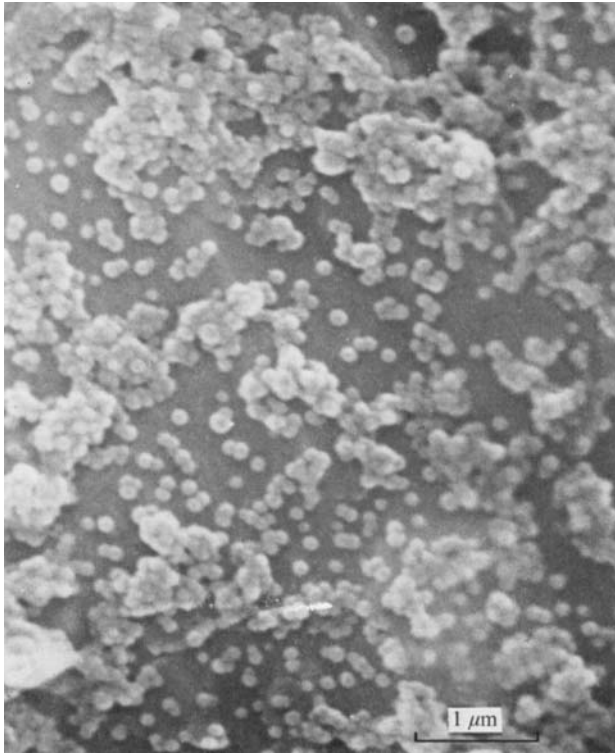FIGURE 9. Photomicrograph of particles for hexatriacontane–water system at 76·5 °C and after 0·03 min irradiation.

FIGURE 12. Photomicrograph of particles for styrene–water system at 10 °C and
after 15 min irradiation. $\bar{D} = 0.10\ \mu m$.